Am J Transl Res 2021;13(2):719-731
www.ajtr.org /ISSN:1943-8141/AJTR0121595

Original Article

Smad7 suppresses melanoma lung metastasis by impairing Tregs migration to the tumor microenvironment

Deliang Ma[1*], Li Qiao[1*], Bingnan Guo[2,3]

[1]Department of Oncology, Linyi Central Hospital, Linyi 276400, Shandong, China; [2]Jiangsu Institute of Health Emergency, Xuzhou Medical University, Xuzhou, Jiangsu, China; [3]Department of Emergency Medicine, The Affiliated Hospital of Xuzhou Medical University, Xuzhou 221000, Jiangsu, China. [*]Equal contributors.

Received September 2, 2020; Accepted December 18, 2020; Epub February 15, 2021; Published February 28, 2021

Abstract: Transforming growth factor β (TGF-β) signaling plays critical roles in both physiological and pathological conditions. In the tumor microenvironment, TGF-β are well demonstrated as a tumor inducer, which also promote tumor growth and metastasis. SMAD family is an important TGF-β signalling transducer, which consists of receptor-regulated SMADs (R-SMADs), common-mediator SMADs (co-SMADs), and inhibitory SMADs (I-SMADs). Smad7 is one of the I-SMADs which has been proved to block TGF-β signalling transduction in both tumor cells and immune cells. Accumulated evidence has suggested SMAD7 acted as a tumor suppressor in various cancer types, such as colorectal cancer, pancreatic cancer and skin melanoma, etc. However, the role of SMAD7 in melanoma lung metastasis has not been well studied. Here, we first investigated the role of SMAD7 on tumor cell viability by overexpressing SMAD7 in murine melanoma cell line B16-F10. Our results showed that SMAD7 overexpression slightly impaired B16-F10 cells growth, promoted cell apoptosis and arrested the cell cycle at S phase. *In vivo* study showed that SMAD7 overexpression inhibited B16-F10 lung metastasis. Further mechanism study suggested that SMAD7 promoted T cells activation by decreasing regulatory T cells (Tregs) infiltrating into the tumor microenvironment. In summary, our results proved that tumor cell derived SMAD7 inhibited melanoma lung metastasis by impairing the migration capacity of Tregs.

Keywords: SMAD7, melanoma, Tregs, metastasis

Introduction

Melanoma is one of the most deadly cancer worldwide, with a 5-year survival rate of only 15%-20% [1]. Melanoma is originated from melanocytes, and can be cured by surgical resection if diagnosed at early stage. However, patients with advanced or metastatic melanoma respond poorly to conventional treatments, such as surgery, chemotherapy and radiotherapy [2]. Recently, the critical role of inflammation in carcinogenesis has been well recognized and several novel immunotherapies against melanoma have shown promising clinical outcome. For example, FDA-approved drugs, the BRAF inhibitors (Vemurafenib and Dabrafenib) and MEK inhibitors (Trametinib and Cobimetinib), showed prolonged survival rate for treating advanced-stage melanoma patients with BRAF-V600-mutant [3, 4]. However, the overall outcome is still unsatisfied [5]. Thus, it's urgent to reveal the detailed mechanism of advanced/metastatic melanoma development and identify new immune therapeutic targets.

Transforming growth factor β (TGF-β) is a superfamily consists of structurally related proteins, including TGF-βs, BMPs (bone morphogenic proteins), activins, inhibins and GDFs (nodal and differentiation factors). These are important cytokines with broad activity, they could affect cell proliferation, migration as well as programmed cell death at cell level [6-8]; they could also regulate immune responses, stress induced tissue responses as well as carcinogenesis at organism level [9-11]. The TGF-β signalling pathway was triggered by the binding of TGF-β ligand with its cell surface

transmembrane receptors. So far, three TGF-β ligands (TGF-β1, TGF-β2 and TGF-β3) and three TGF-β receptor complexes (TGF-β type I receptors, TGF-β type II receptors, TGF-β type III receptors) have been identified [12].

The SMAD proteins are important components of the TGF-β signalling pathway, which transduce the extracellular signals to the nucleus [13]. Up to now, eight different SMAD proteins are discovered, which can be categorised into three groups: 1) R-SMAD (the receptor-regulated SMAD), including SMAD1, SMAD2, SMAD3, SMAD5, and SMAD8/9; 2) Co-SMAD (the common-mediator SMAD), including SMAD4 solely; 3) I-SMAD (the inhibitory SMAD), including SMAD6 and SMAD7. The binding of extracellular TGF-β to its type II receptor will phosphorylate the type I receptor at specific serine and threonine residues. The TGF-β, TGF-β type I receptors, TGF-β type II receptors triple complex will transduce the canonical signalling pathway by phosphorylating its downstream target proteins SMAD2/3. Then the phosphorylated SMAD2/3 will form a heterodimeric complex with SMAD4, and subsequently translocate to the nucleus to regulate the downstream target genes expressions [14]. The transduction of TGF-β signalling is regulated by the inhibitory activity of SMAD7. Under steady state, SMAD7 is retained in the nucleus of the cells. However, upon activation of TGF-β signalling, SMAD7 would move to the cytoplasm to inhibit TGF-β mediated SMAD2/SMAD3 phosphorylation. Thus, SMAD7 is known as a negative feedback regulator to control TGF-β responses [15].

The role of SMAD7 in carcinogenesis has been studied during the past decades. It has been proved that SMAD7 acted as a tumor suppressor in various cancer types. For example, SMAD7 could suppress HCC (hepatocellular carcinoma) development by inhibiting the G1-S phase transition of tumor cells [16]; overexpression of SMAD7 in T cell inhibited the growth of colitis-associated CRC (colorectal cancer) [17]. However, the role of SMAD7 in melanoma lung metastasis has not been well documented. Besides, the effects of SMAD7 in the antitumor immune responses are still largely unknown.

Here, for the first time we reported that tumor derived SMAD7 could suppress melanoma lung metastasis in murine B16-F10 lung metastasis model. Mechanism study proved that SMAD7 overexpression could promote anti-tumor T cell activity and cytokines production. Further *in vitro* and *in vivo* studies demonstrated that SMAD7 impaired the Tregs migration to the local tumor microenvironment, thus inhibiting the immunosuppressive function of Tregs. Collectively, our study showed that SMAD7 was a promising therapeutic target against tumor metastasis.

Materials and methods

Experimental animals

6-8 weeks old specific pathogen-free (SPF) female C57BL/6 mice were purchased from the Experimental Animal Center of Shandong University (Jinan, China). Upon arrival, mice were group housed in specific pathogen-free facilities (room temperature 25 ± 2°C; a 12/12 h light/dark cycle). Animal handling and experimental procedures were conducted strictly in accordance with the Provision and General Recommendation of Chinese Experimental Animal Administration Legislation and approved by the Science and Technology Department of Shandong Province.

Plasmid construction

Full-length murine SMAD7 DNA sequences were cloned from mouse PBMCs by polymerase chain reaction (PCR) and subcloned into pcDNA3.1 expression vector (Invitrogen, Carlsbad, CA). The B16-Mock and B16-SMAD7 overexpression cells were generated by transfection of pcDNA3.1 empty vector or pcDNA3.1-SMAD7 into B16-F10 cells using Lipofectamine 3000 (Thermo Fisher Scientific, Waltham, MA) according to the manufacturer's protocol. 48 hours later, cells were harvested for Western blot to confirm the successfully transfection of SMAD7 into the cells. For further experiments, two type transfection B16-10 cells were conducted selection with neomycin (1 mg/ml, Invitrogen, Carlsbad, CA) for stable expression.

Cell culture

Murine skin melanoma cell line B16-F10 was obtained from American Type Culture Collection (Manassas, VA). The cells were cultured in complete DMEM medium (Hyclone, Piscataway, NJ), containing 10% FBS (GIBCO, Waltham, MA) and 1% Penicillin-Streptomycin antibiotics (Sigma Aldrich, St. Louis, MO). Cells were incubated at 37°C with 5% Carbon Dioxide (CO_2).

Western blot

B16-Mock and B16-SMAD7 cells were lysed, total protein was extracted using the NP40 lysis buffer system (Thermo Fisher Scientific, Waltham, MA) mixed with PhosSTOPTM (Roche, Basel, Switzerland) and Complete ULTRA Tablets (Roche, Basel, Switzerland). Protein quantification was done by using PierceTM BCA Protein Assay Kit (Thermo Fisher Scientific, Waltham, MA). Samples were then mixed with loading dye and separated by 12% SDS-PAGE gel, transferred onto 0.2 μm polyvinylidene difluoride (PVDF) transfer membranes (Thermo Fisher Scientific, Waltham, MA), blocked in 5% milk in PBST, and incubated overnight with the rabbit polyclonal anti-mouse SMAD7 antibody (42-0400, Thermo Fisher Scientific, Waltham, MA). Followed by incubation with horse radish peroxidase (HRP)-conjugated goat anti-rabbit IgG (sc-2004; Santa Cruz, Dallas, TX) for 2 hours at room temperature. Finally, signals were detected using the Elite ECL Reagents (Cell Signalling Technology, Danvers, MA) according to the manufacturer's protocol., Rabbit polyclonal anti-mouse β actin antibody (ab-8227, Abcam, Cambridge, United Kingdom) was used as housekeeping gene control.

Ki67 staining

1×10^5 B16-Mock or B16-SMAD7 cells resuspended in complete DMEM medium were seeded in 6-well plates and cultured for 24 hours. Cells were harvested and washed with PBS twice. Then cells were fixed with ice-cold 70% ethanol and incubator in -20°C for 1 hour. Later, cells were washed with PBS and stained with APC-conjugated Ki67 antibody (clone 16A8, Biolegend, San Diego, CA) for 20 min at room temperature. Finally, cells were collected and detected by LSRFortessa™ cytometry (BD Biosciences, San Jose, CA). The FACS data were further analyzed by Flowjo software (FlowJo LLC, Ashland, Oregon).

Apoptosis assay

1×10^5 B16-Mock or B16-SMAD7 cells resuspended in complete DMEM medium were seeded in 12-well plate and cultured overnight. The next day, the medium was replaced with DMEM medium containing 2% FBS to induce cell apoptosis. 24 hours Laster, cells were harvested and apoptosis assay was performed using the Apoptosis Detection Kit (Biolegend, San Diego, CA). Briefly, cells were collected and resuspended in AnnexinV binding buffer. Then APC-conjugated AnnexinV and DAPI (4',6-Diamidino-2-Phenylindole, Dilactate) were added in to the cells and incubated for 15 min at 4°C in the dark. The distribution of the $AnnexinV^+$ $DAPI^-$ early apoptotic and $AnnexinV^+$ $DAPI^+$ late apoptotic cells were detected by BD LSRFortessa™ cytometry and analyzed by Flowjo software.

Cell cycle assay

1×10^5 B16-Mock or B16-SMAD7 cells resuspended in complete DMEM medium were seeded in 6-well plates and cultured for 24 hours. The cells were harvested with the same method as Ki67 staining. The cells were stained with Propidium Iodide Solution (Biolegend, San Diego, CA) and detected by LSRFortessa™ cytometry. The FACS data were further analyzed by Flowjo software.

Animal model

To establish murine melanoma lung metastasis model, mice were intravenously injected with 4×10^5 B16-Mock or B16-SMAD7 cells. Two weeks later, mice were sacrificed and lungs were removed, and the metastatic nodules were quantified. For T cells depletion assay, one day prior to the tumor injection, mice were i.p. injected with 500 mg anti-CD3 antibody (clone 17A2, Bioxcell, Lebanon, NH), the antibody injections were repeated every three days.

Flow cytometry analysis

Splenocytes were isolated from tumor-bearing mice, tumor infiltrating lymphocytes were isolated from the lung 2 weeks after tumor inoculation. 1×10^6 solenocytes or TILs were seeded into flow tube and incubated with fluorescence-conjugated antibodies for 30 min at 4°C in dark. After three round of washing with staining buffer, the samples were assessed by LSRFortessa™ X-20 cytometry. The antibodies used were BV421 anti-mouse CD3 (Clone 17A2, Biolegend, San Diego, CA), FITC anti-mouse CD4 (Clone GK1.5, Biolegend, San Diego, CA), PE anti-mouse CD8 (53-6.7, Biolegend, San Diego, CA), PE-CF594 anti-mouse CD3 (Clone 145-2C11, BD Biosciences, San Jose, CA), APC anti-mouse CD44 (Clone IM7, Biolegend, San Diego, CA), Alexa Fluor 700 anti-mouse CD62L (Clone MEL-14, Biolegend, San Diego, CA), BV421 anti-mouse FoxP3 (Clone MF-14,

Biolegend, San Diego, CA), APC anti-mouse CD25 (Clone 3C7, Biolegend, San Diego, CA), PerCP/Cyanine5.5 anti-mouse TNF-α (Clone MP6-XT22, Biolegend, San Diego, CA), Alexa Fluor 700 anti-mouse IFN-γ (Clone XMG1.2, Biolegend, San Diego, CA). The FACS data were further analyzed by Flowjo software.

In vitro Tregs differentiation

Naïve $CD4^+$ T cells were sorted form mouse spleen using the Naive T Cell Isolation Kit (Miltenyi Biotec, Bergisch Gladbach, Germany) according to the manufacturer's protocol. Cells were then seeded into anti-CD3 (Clone 145-2C11, BioLegend, San Diego, CA) pre-coated 24 well plate in the presence of soluble anti-CD28 (Clone 37.51, BioLegend, San Diego, CA). Then cells were treated with 5 μg/ml anti-IFN-γ (Clone XMG1.2, Bioxcell, Lebanon, NH), 50 U IL-2 (Miltenyi Biotec, Bergisch Gladbach, Germany) and 3 ng/ml TGF-β (Peprotech, Rocky Hill, NJ). Supernatants from B16-Mock and B16-SAMD7 cells were added into the culture medium, respectively. 72 hours later, cells were harvested for FoxP3 staining.

Treg suppression assay

1×10^5 naïve $CD4^+$ T cells were sorted using the Naive T Cell Isolation Kit, labelled with CFSE (Thermo Fisher Scientific, Waltham, MA) and cultured in a 96-well round bottom plate with anti-CD3/CD28-conjugated beads (Thermo Fisher Scientific, Waltham, MA). In vitro differentiated Tregs were added into the cells at the ratio of 1:1. Another 72 hours later, cells were collected and proliferation rate was detected by LSRFortessa™ X-20 cytometry and analyzed by Flowjo software.

RNA extraction and real time polymerase chain reaction (RT-PCR)

B16-Mock and B16-SMAD7 cells were collected and total RNA was extracted with RNA isolation kit (Macherey-Nagel, Germany) according to the manufacturer's instructions. SuperScript III (Thermo Fisher Scientific, Waltham, MA) was used to synthesis the first strain cDNA. The purity and concentration of the cDNA was measured by NanoDrop (Thermo Fisher Scientific, Waltham, MA). SYBR Green were used in the PCR Master Mix (Promega, Madison, WI). Primers used are mouse *ccl1* forward: 5-CGTGTGGATACAGGATGTTGACAG-3, mouse *ccl1* reverse: 5-AGGAGGAGCCCATCTTTCTGTAAC-3; *ccl3* forward: 5-TGAATGCCTGAGAGTCTTGG-3, *ccl3* reverse: 5-TTGGCAGCAAACAGCTTATC-3; *ccl5* forward: 5-CACCACTCCCTGCTGCTT-3, *ccl5* reverse: 5-ACACTTGGCGGTTCCTTC-3; *cxcl12* forward: 5-TGCATCAGTGACGGTAAACCA-3, *cxcl-12* reverse: 5-TTCTTCAGCCGTGCAACAATC-3; *ccl17* forward: 5-CAAGCTCATCTGTGCAGACC-3, *ccl17* reverse: 5-CGCCTGTAGTGCATAAGAGTCC-3; *ccl20* forward: 5-GCCTCTCGTACATACAGACGC-3, *ccl20* reverse: 5-CCAGTTCTGCTTTGGATCAGC-3; *ccl22* forward: 5-AAGACAGTATCTGCTGCCAGG-3, *ccl22* reverse: 5-GATCGGCACAGATATCTCGG-3; *GAPDH* forward: 5-CTCATGACCACAGTCCATGC-3, *GAPDH* reverse: 5-CACATTGGGGGTAGGAACAC-3.The expression of GAPDH was used for sample normalization. Gene expression was measured by the $2^{-\delta\delta Ct}$ method.

ELISA

1×10^5 B16-Mock and B16-SMAD7 cells were seeded into 6-well plate and cultured for 2 days. Cell supernatants were collected and ELISA was performed to detect the CCL5 production (Thermo Fisher Scientific, Waltham, MA) according to the manufacturer's protocol. The level of CCL5 in the supernatants was quantified based on the standard curve.

Tregs migration assay

Migration assays were performed using 96-well Transwell plates with a 5.0 μm polycarbonate membrane (Corning Life Sciences, New York). Briefly, 1×10^6 *in vitro* differentiated Tregs were seeded to the top chamber. Supernatants from B16-Mock or B16-SMAD7 were added to the bottom chamber. After 4 hours, migrated cells in the lower chamber were counted, migration index was calculated. For CCR5 blocking, *in vitro* differentiated Tregs were incubated overnight with either 1 μM Maraviroc (Sigma Aldrich, St. Louis, MO) or DMSO vehicle, prior to the transwell assay.

Statistical analysis

All data were analyzed with one-way ANOVA and were expressed as means ± SD; data were analyzed using GraphPad Prism 7 software for Windows (GraphPad, company, San Diego, CA) and differences were considered statistically significant when $P < 0.05$. The significance levels are marked *, $P < 0.05$; **, $P < 0.01$; ***, $P < 0.001$.

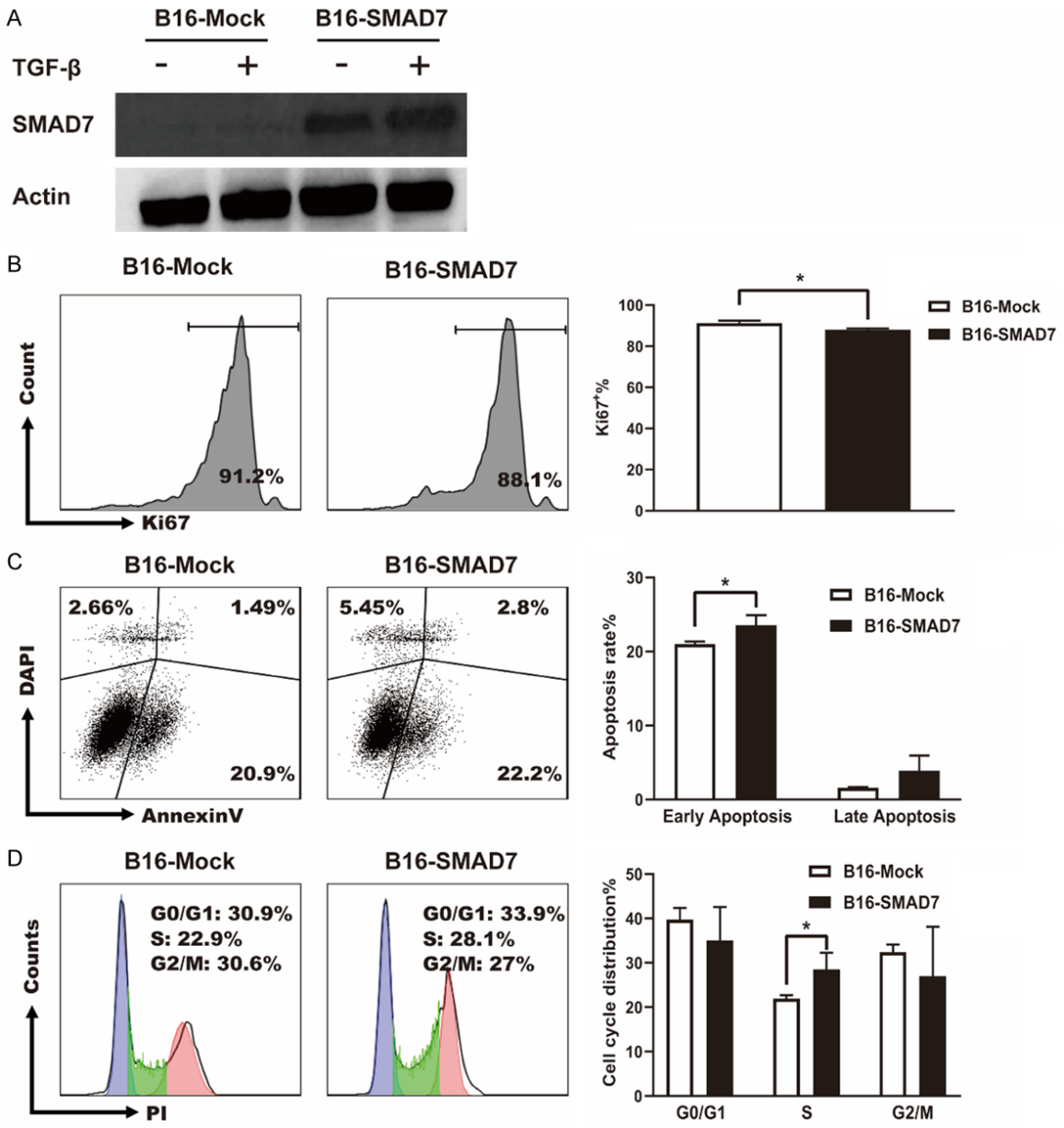

Figure 1. SMAD7 slightly affected B16-F10 cells viability by arresting cell cycle at S phase. A. 2×10^6 B16-Mock or B16-SMAD7 cells were seeded into 6-well plate in the presence of 1 ng/ml recombinant TGF-β or PBS. 8 hours later, cells were harvested for western blot to detected the SMAD7 expression. Actin was used as control. B. Representative images of Ki67 staining assay. 1×10^5 B16-Mock or B16-SMAD7 cells were seeded into 6-well plate and cultured for 24 hours. The expression of the proliferate marker Ki67 was assessed by flow cytometry. C. Representative images of apoptosis assay. 1×10^5 B16-Mock or B16-SMAD7 cells were cultured in DMEM containing 2% FBS for 24 hours. The apoptosis rates were assessed by AnnexinV & DAPI staining. The early apoptotic cells were defined as AnnexinV$^+$ DAPI$^-$, the late apoptotic cells were defined as AnnexinV$^+$ DAPI$^+$. D. Representative images of cell cycle assay. 1×10^5 B16-Mock or B16-SMAD7 cells were seeded in 6-well plate. 24 hours later, cells were harvested, fixed in ice-cold ethanol and stained with PI. The percenatges of cells in each cell division phase was shown. Data are presented as means ± SD. *$P < 0.05$.

Results

SMAD7 slightly affected tumor cell viability

To dissect the role of SMAD7 in carcinogenesis: We first assessed the expression level of SMAD7 in B16-F10 cells. Western blot results showed that the endogenous expression of SMAD7 in B16-F10 cells was at a relatively low level (**Figure 1A**). Thus, we overexpressed SMAD7 by transfection B16-F10 cells with PCDNA3.1 vector encoding SMAD7 or mock as

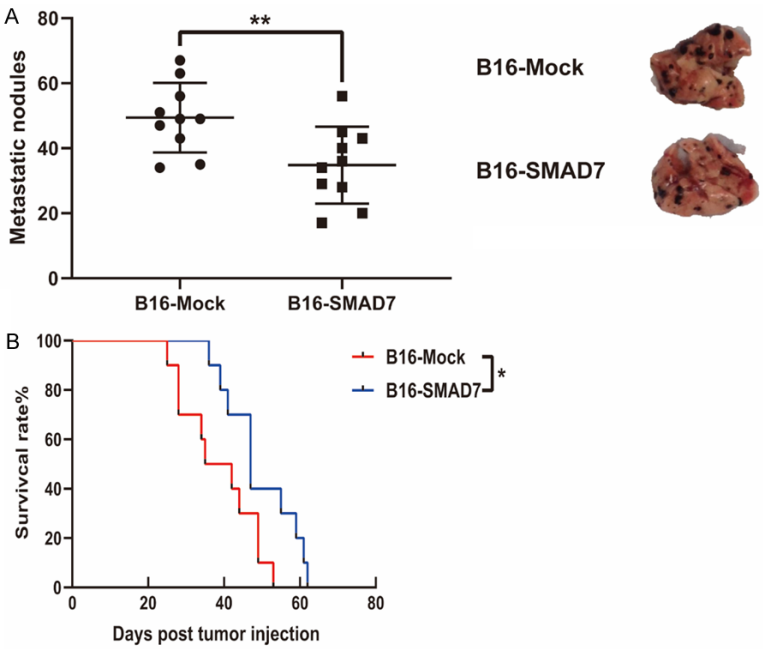

Figure 2. SMAD7 suppressed B16-F10 lung metastasis and prolonged survive. A. Mice were intravenously injected with 4×10^5 B16-Mock or B16-SMAD7 cells. Two weeks later, mice were sacrificed, lungs were removed, and the metastatic nodules were quantified. B. The survival rate of B16-F10 tumor bearing mice were monitored. Survival was monitored and compared by log-rank test. The data shown are representative of three experiments. Data are presented as means ± SD. *P < 0.05, **P < 0.01.

SMAD7 suppressed B16-F10 lung metastasis by promoting T cell activation

B16-F10 lung metastasis models were established by i.v. injection of B16-Mock and B16-SMAD7 cells into the mice to study the effect of SMAD7 on carcinogenesis *in vivo*. SMAD7 overexpression in B16-F10 cells significantly suppressed B16-F10 lung metastasis, identified by less metastatic nodules in the lung (**Figure 2A**). Survival curve also proved that mice receiving B16-SMAD7 injection displayed longer survival time post tumor injection. The average survival rate increased from 38.7 d in B16-Mock group to 49.4 d in B16-SMAD7 group (**Figure 2B**). These results demonstrated that SMAD7 acted as a tumor suppressor in murine B16-F10 melanoma lung metastasis model.

control. The results showed that SMAD7 was successfully transfected into B16-F10 cells (**Figure 1A**). Adding recombinant TGF-β slightly increased the SMAD7 expression in both B16-Mock and B16-SMAD7 cells, however the difference is quite minimal (**Figure 1A**).

Next, we evaluated the effects of SMAD7 on tumor cell viability *in vitro*. Ki67 staining was carried out to assess the cell proliferation ability and the results showed that B16-F10 grew very aggressively and SMAD7 slightly inhibited B16-F10 cells proliferation (**Figure 1B**). Apoptosis assay proved that SMAD7 promoted B16-F10 cells apoptosis. The early apoptosis rate increased from 21 ± 0.08% to 23.6 ± 1.12%, however the difference was still minimal (**Figure 1C**). Cell cycle analysis showed that more cells were stuck at S phase in B16-SMAD7 cells (**Figure 1D**). Overall, these results indicated that SMAD7 inhibited B16-F10 cells proliferation and promoted B16-F10 cells apoptosis by arresting the cell cycles at S phase. Notably, the overall effects of SMAD7 on B16-F10 cells viability were quite minimal.

It is unlikely that the minimal effects of SMAD7 on B16-F10 cell viability could lead to such significant difference *in vivo*. To further study the mechanism of how SMAD7 suppressed B16-F10 lung metastasis *in vivo*, splenocytes and TILs (tumor infiltrating lymphocytes) were isolated and flow cytometry staining were performed. We found that SMAD7 didn't affect the percentage of total T cells, $CD4^+$ T cells and $CD8^+$ T cells in both spleen and TILs (**Figure 3A** and **3B**). Moreover, the activation status of T cells in spleen also showed no difference (Figure S1A). Interestingly, we found that the percentages of effector $CD3^+$ T cells and $CD8^+$ T cells were increased in the lung, while the percentage of naïve $CD4^+$ T cells were decreased, suggesting that SMAD7 promoted T cells activation in the tumor microenvironment (**Figure 3C**).

T cells play a vital role in the anti-tumor immune responses. To further elucidate the effect of SMAD7 on T cells activation *in vivo*. Splenocytes and TILs harvested from tumor-bearing mice were stimulated with PMA and ionomycin for four hours, the effector cytokines (mainly TNF-α

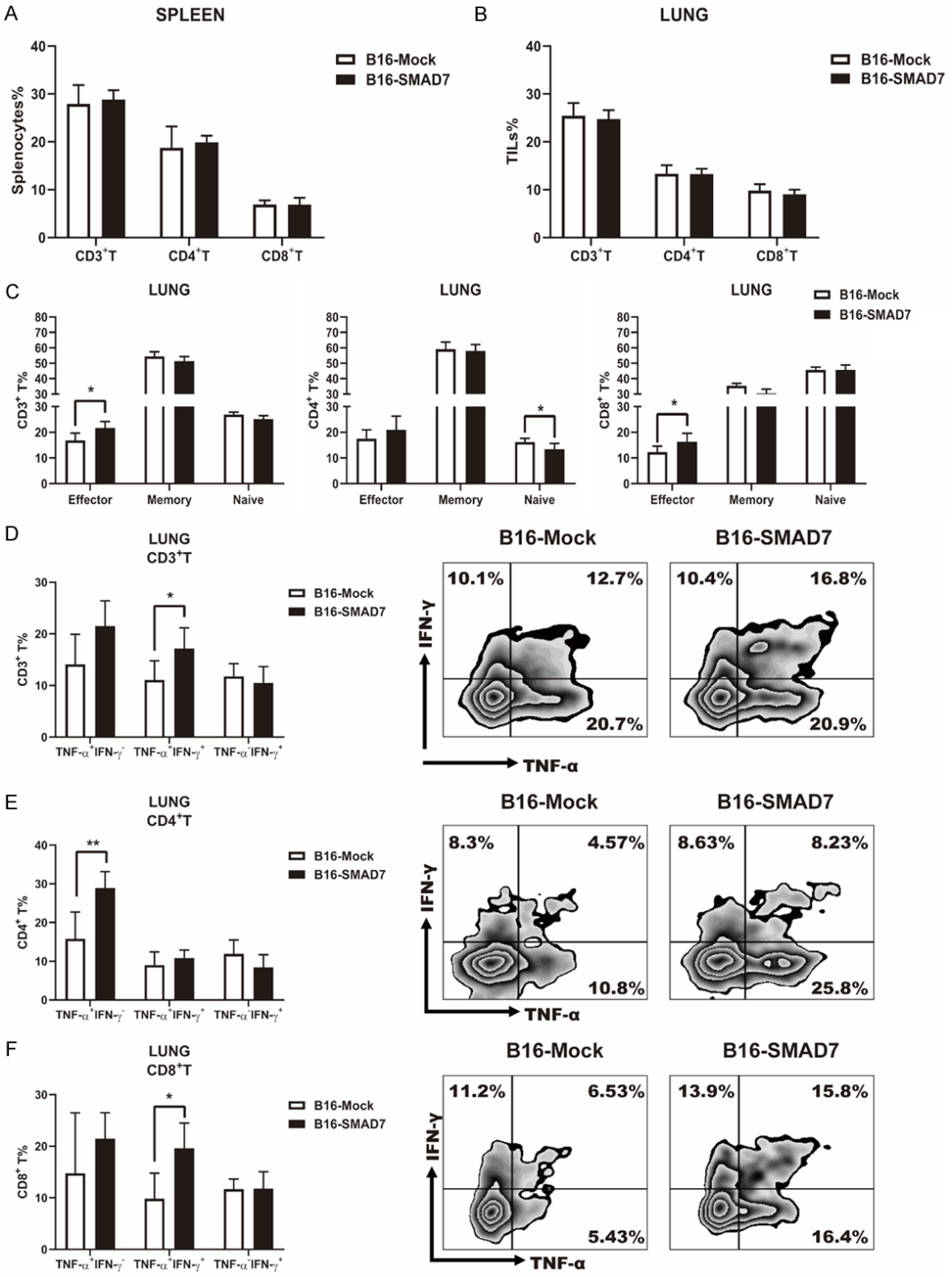

Figure 3. SMAD7 promoted T cells activation and effector cytokines prodcution in the lung. (A) Splenocytes and (B) tumor infiltrating lymphocytes (TILs) were isolated from tumor bearing mice 2 weeks after tumor injection. The percentages of $CD3^+$ T cells, $CD4^+$ T cells and $CD8^+$ T cells were detected by flow cytometry. (C) The percentages of $CD44^+CD62L^-$ effector, $CD44^+CD62L^+$ memory and $CD44^-CD62L^+$ naïve T cell subsets were detected by flow cytometry. Representative images of TNF-α^+ IFN-γ^-, TNF-α^+ IFN-γ^+, TNF-α^- IFN-γ^+ (D) $CD3^+$ T cells, (E) $CD4^+$ T cells and (F) $CD8^+$ T cells in the TILs are shown. Data are presented as means ± SD. *P < 0.05, **P < 0.01.

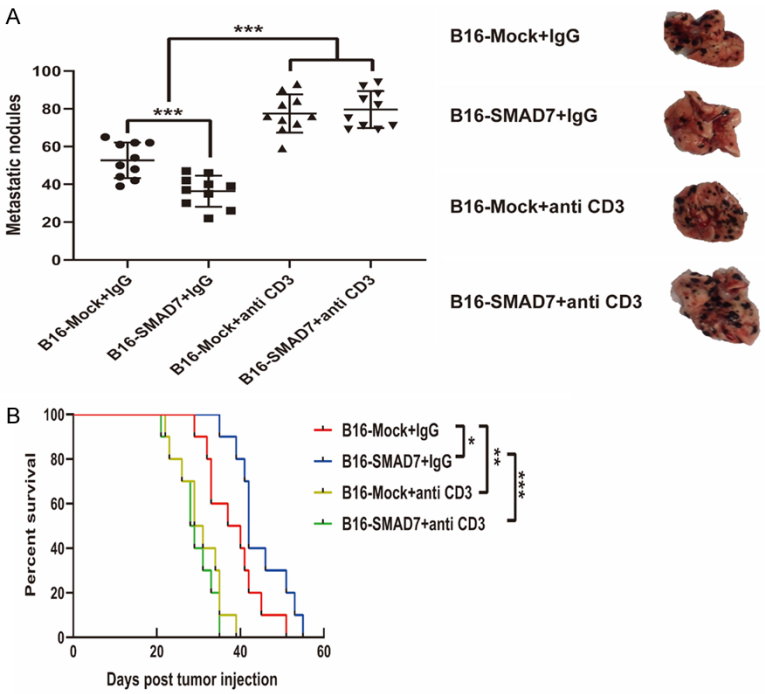

Figure 4. The anti-tumor activity of SAMD7 was T cells dependent. Mice were i.p injected with anti-CD3 antibody or IgG control one day before tumor injection. A. Two weeks later, mice were sacrificed and lungs were removed, and the metastatic nodules were quantified. B. The survival rate of B16-F10 tumor bearing mice were monitored. Survival was monitored and compared by log-rank test. The data shown are representative of three experiments. Data are presented as means ± SD. $*P < 0.05$, $**P < 0.01$, $***P < 0.001$.

and IFN-γ) were assessed by flow cytometry. The results showed that the percentages of TNF-α$^+$ IFN-γ$^+$ T cells in the TILs were increased in the B16-SMAD7 group, from 11.06 ± 3.75% in the B16-Mock group to 17.16 ± 4.02% in the B16-SMAD7 group (**Figure 3D**); the percentages of TNF-α$^+$ IFN-γ$^-$ CD4$^+$ T cells were increased in the B16-SMAD7 group, from 15.78 ± 6.94% in the B16-Mock group to 28.48 ± 4.81% in the B16-SMAD7 group (**Figure 3E**); the percentages of TNF-α$^+$ IFN-γ$^+$ CD8$^+$ T cells in the TILs were increased in the B16-SMAD7 group, from 9.8 ± 4.99% in the B16-Mock group to 19.6 ± 4.88% in the B16-SMAD7 group (**Figure 3E**). On the other hand, the effector cytokines expression of T cells in spleen showed no significant difference (Figure S1B-D). Taken together, our data suggested that SMAD7 suppressed B16-F10 lung metastasis through enhancing T cell activation.

The tumor suppressive function of SMAD7 was T cell dependent

The previous results proved that SMAD7 could inhibit B16-F10 lung metastasis by activating T cells. To further confirm the role of T cells in SMAD7-mediated tumor suppressive function, we depleted T cells in the tumor-bearing mice. After T cells depletion, the anti-tumor activity of SMAD7 was diminished (**Figure 4A**). The mice also showed comparable survival rate after T cells depletion in B16-Mock and B16-SMAD7 groups (**Figure 4B**). These results demonstrated that the anti-tumor activity of SMAD7 was T cells dependent.

SMAD7 impaired Treg migration to the tumor microenvironment

Our previous results proved that SMAD7 promoted the local T cell dependent anti-tumor immune responses, suggesting that T cell function was suppressed in the tumor microenvironment. The tumor-promoting role of Tregs has been well recognized by suppressing anti-tumor immune responses [18]. Thus, we assessed the Tregs distribution in spleen and TILs. We found that SMAD7 didn't affect the percentage of Tregs in the spleen (Figure S2A). Interestingly, we found that the percentage of Tregs in the TILs was significantly decreased in the B16-SMAD7 mice (**Figure 5A**).

To assess the origin of the Tregs in the TILs. We performed *in vitro* Tregs differentiation assay by adding TGF-β into the freshly isolated naive CD4$^+$ T cells to induce Tregs differentiation as previously described [19]. Meanwhile, we also added cell culture supernatants collected from B16-Mock (B16-Mock SUP) and B16-SAMD7 (B16-SMAD7 SUP), respectively. We found that B16-SMAD7 SUP treatment induced similar level of Tregs compared to the B16-Mock SUP, suggesting SMAD7 didn't affect Tregs differentiation (**Figures 5B** and S2B). We further assessed the T cell suppressive function of Tregs induced by B16-Mock SUP and B16-SMAD7 SUP. By co-culturing the Tregs with freshly isolated CD4$^+$ T cells, we found that SMAD7 had no influence on

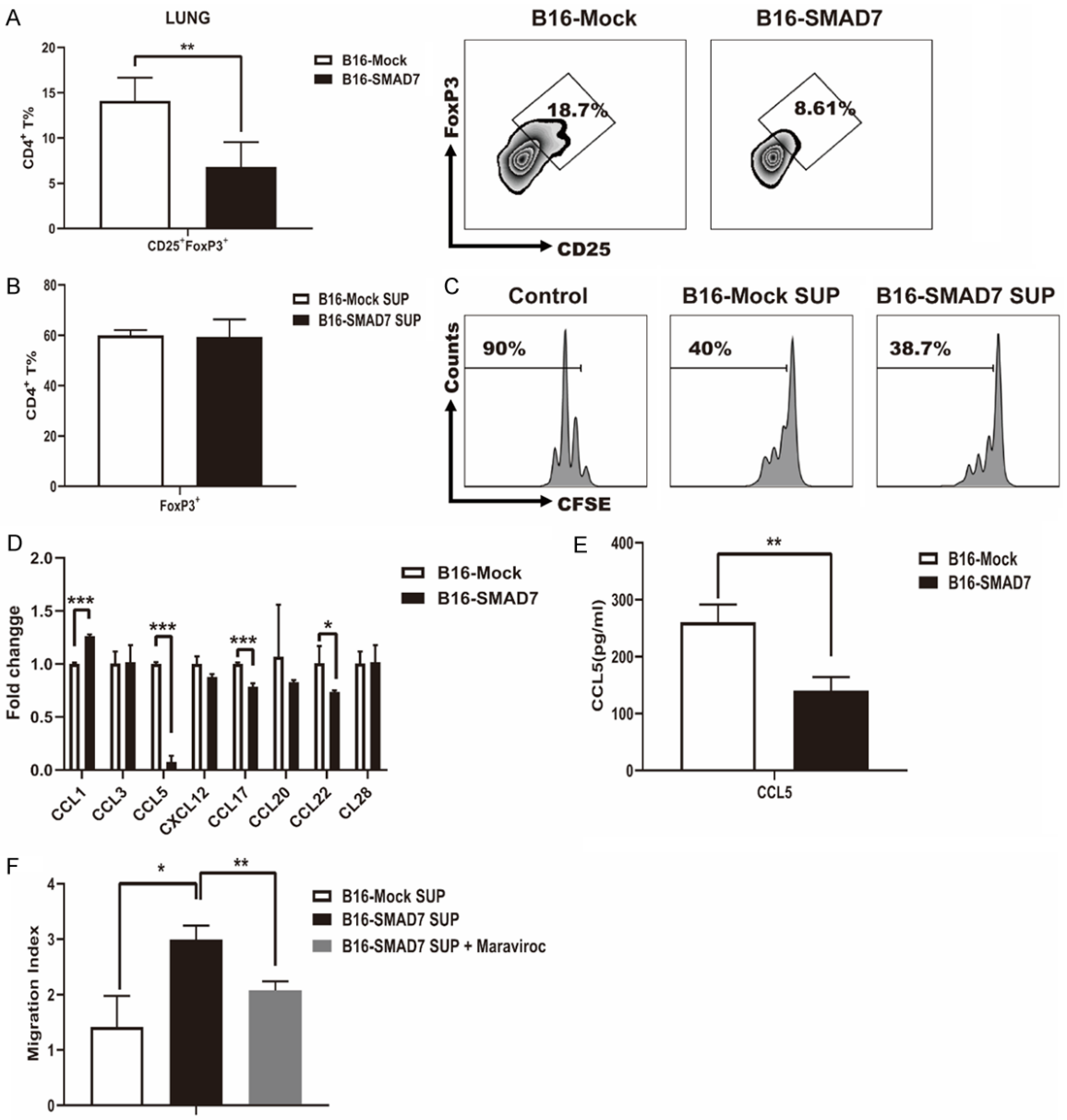

Figure 5. SMAD7 impaired Tregs migration to the tumor microenvironment. A. Representative images of $CD4^+CD25^+FoxP3^+$ Tregs presented in the TILs. B. Naïve $CD4^+$ T cells were treated with anti-IFN-γ, IL-2, TGF-β and supernatants from B16-Mock or B16-SMAD7 to induce differentiation into Tregs. The percentages of $FxoP3^+$ Tregs were shown. C. Representative images of CFSE labelled $CD4^+$ T cells after co-culture with Tregs. D. qPCR results for *ccl1*, *ccl3*, *ccl5*, *cxcl12*, *ccl17*, *ccl20*, *ccl22*, *ccl28* between B16-Mock and B16-SAMD7 cells. E. The secretion of CCL5 in B16-Mock and B16-SAMD7 cells were assessed by ELISA. F. Migration index of Tregs attracted by supernatants form B16-Mock or B16-SMAD7. Maraviroc was added to block the CCR5 chemotaxis. Data are presented as means ± SD. $*P < 0.05$, $**P < 0.01$, $***P < 0.001$.

the T cell suppressive capacity of Tregs (**Figure 5C**).

Tregs are known to migrate rapidly in response to chemokines produced at the tumor microenvironment, including CCL1, CCL3, CCL5, CXCL12, CCL17, CCL20, CCL22, CCL28 [20, 21]. Thus, we hypothesised that SMAD7 impaired Tregs migration to the tumor microenvironment by downregulation chemokines expressions. Indeed, we found that B16-SMAD7 showed less CCL5, CCL17, CCL22 expression in which CCL5 showed dramatic downregulation of nearly 10 folds (**Figure 5D**). The down-

regulation of CCL5 in the B16-SMAD7 cells was further confirmed by Elisa, the results showed that SMAD7 decreased the CCL5 production in B16-F10 cells (**Figure 5E**). To further confirm that SMAD7 impaired Tregs migration, we performed transwell assay *in vitro*. The results showed that supernatant collected from B16-SMAD7 cells significantly impaired the Tregs migration (**Figure 5F**). To further prove the Tregs migration was dependent on CCL5, Maraviroc, a CCR5-specific inhibitor was used to block the CCL5/CCR5 chemotaxis. The transwell results showed that Maraviroc reduced the Tregs migration to the comparable level of B16-Mock SUP group. Collectively, these results suggested that SMAD7 promoted the anti-tumor T cell activity by blocking Tregs migration to the tumor microenvironment.

Discussion

In the present study, we found that overexpression of SMAD7 in B16-F10 cells slightly affected cell viability, at least to some extent. *In vivo* study revealed that SMAD7 overexpression significantly suppressed B16-F10 lung metastasis and prolonged the survival rate. Detailed mechanism study showed that SMAD7 could promote the anti-tumor activity by enhancing T cells activation. Further investigation proved that SMAD7 impaired Tregs migration to the tumor microenvironment in an CCL5/CCR5 dependent manner, thus inhibiting the T cell suppressive function of Tregs.

The role of TGF-β signalling in tumor progression has been well documented. In the early stage of carcinogenesis, TGF-β signalling exerts antitumorigenic functions, while at later stages, TGF-β signalling exerts protumorigenic functions [22]. The role of TGF-β signalling in B16-F10 lung metastasis has also been reported by different groups: TGF-β signalling could promote B16 lung metastasis by enhancing the tumor epithelial-mesenchymal transition [23]; myeloid cells derived TGF-β signalling activation was essential for B16 lung metastasis [24]; TGF-β signalling induced an immune suppressive tumor microenvironment to promote tumor cells metastasis to the lung [25]. Thus, targeting TGF-β signalling is a promising therapeutic strategy against tumor lung metastasis. Indeed, blocking TGF-β signnalling with small inhibitors or genetic modification has been reported to bypass the immunosuppressive microenvironment to promote anti-tumor immune responses [26, 27].

The SMAD proteins are components of TGF-β signalling pathway, which played important roles during carcinogenesis [28, 29]. Targeting SMAD proteins has shown promising outcome for cancer treatment [30]. SMAD7, together with SMAD6 are inhibitory SMAD that could block the TGF-β signalling pathway. Unlike other members in SMAD family, the role of SMAD7 in the tumor progression has not been well documented. SMAD7 deficiency showed higher incidence and multiplicity in murine HCC model [16]; SMAD7 overexpression in human melanoma cell lines impaired the bone metastasis by reducing the expression of parathyroid hormone-related protein, IL-11 and connective tissue growth factor [31]; overexpression of SMAD7 in T cells associated with severe colitis and reduced the growth of CRC (colorectal cancer) [17]. However, the detailed role and mechanism of SMAD7 in melanoma lung metastasis are still unclear.

We found SMAD7 was expressed at a relatively low level in B16-F10 cells. *In vitro* study found that SMAD7 overexpression slightly affected B16-F10 cells viability, however the influence was quite minimal. This result indicated that SMAD7 acted as a direct tumor suppressor in B16-F10 cells, which was similar to previous studies utilizing breast cancer cell line and HCC cell line [16, 32]. Collectively, our data and other reports indicated that SMAD7 was a general tumor cell suppressor.

T cells played an important role in suppressing tumor lung metastasis through multiple mechanisms [33, 34]. Our *in vivo* study proved that SMAD7 could promote anti-tumor T cell immune responses. Interestingly, after we deplete T cell *in vivo*, the anti-tumor activity of SMAD7 was diminished. This result suggested that although SMAD7 could directly suppress B16-F10 cells growth *in vitro*, this direct inhibition was insufficient to induce significant tumor inhibition *in vivo*. Tumor microenvironment is accompanied with high pressure, lack of oxygen and nutrient, as well as anti-inflammatory cytokines (e.g. IL-10, iNOS, TGF-β) produced by various cell types, including tumor cells, stroma cells, fibroblasts as well as immune cells [35]. We found that in our B16-F10 lung metastasis model, overexpression of SMAD7 reduced the

Tregs infiltration in the local microenvironment. These results demonstrated that SMAD7 promoted local anti-tumor T cell activation through reducing Tregs infiltration. It is noteworthy that Tregs are not the only immune suppressive cells in the tumor microenvironment. Other immune cell, such as TAMs (tumor-associated macrophages), MDSCs (myeloid derived suppressive cells), Bregs (regulatory B cells) could also suppress the T cells function [36-38]. Further studies should be done to investigate the role of SMAD7 on these immune suppressive cells.

The source of Tregs in the local inflammatory site mainly originated from two pathways: 1) local differentiation of $CD4^+$ T cells into Tregs [39]; 2) migrated Tregs from the peripheral lymphoid organ [40]. To understand the reason why Tregs were decreased in B16-SMDA7 group, we conducted experiments based on these two perspectives. We found that conditioned medium from B16-SMAD7 cells didn't affect Tregs differentiation and immunosuppressive function. Notably, we proved that B16-SMAD7 cells produced less chemokines that could attract Tregs into the tumor microenvironment, including CCL5, CCL17, CCL22 [25, 41]. Though CCL1 was upregulated in the B16-SMAD7 cells, the downregulation of CCL5, CCL17, CCL22 synergistically shield the attractive function of CCL1, proved by the transwell assy. Moreover, the enhanced migration of Tregs by SMAD7 was reduced to the basal level when CCL5/CCR5 axis was blocked, suggesting CCL5 played a dominant role in attracting Tregs into the tumor microenvironment. Collectively, these results indicated that SMAD7 impaired the Tregs migration by reducing the chemokines secretion patterns by tumor cells. However, the detailed mechanism of how SMAD7 reduced chemokines productions are still unknown. We hypothesis that SMAD7 overexpression blocked the TGF-β signalling in the tumor cell, thus regulating the chemokines production by the tumor cells. Further studies are needed to be done to test our hypothesis.

Taken together, our results demonstrated SMAD7 played a protective role in melanoma lung metastasis. Tumor derived SMAD7 promoted the T cells mediated anti-tumor activity by impairing the Tregs migration to the tumor microenvironment. Thus, SMAD7 could serve as a potential therapeutic target for metastatic cancer treatment.

Acknowledgements

This work was supported by grants from the Natural Science Foundation of the Jiangsu Higher Education Institutions of China (18KJB-320027), Jiangsu Planned Projects for Postdoctoral Research Funds (2018K247C), Xuzhou Medical University Research Funds (2014KJ12) and Shandong Planned Projects for Traditional Chinese Medicine (2017-474).

Disclosure of conflict of interest

None.

Address correspondence to: Dr. Bingnan Guo, Jiangsu Institute of Health Emergency, Xuzhou Medical University, Xuzhou, Jiangsu, China; Department of Emergency Medicine, The Affiliated Hospital of Xuzhou Medical University, Xuzhou 221000, Jiangsu, China. Tel: +86-516-8580-6067; Fax: +86-516-8580-6067; E-mail: guobingnan@xzhmu.edu.cn

References

[1] Siegel RL, Miller KD and Jemal A. Cancer statistics, 2016. CA Cancer J Clin 2016; 66: 7-30.
[2] Luke JJ, Flaherty KT, Ribas A and Long GV. Targeted agents and immunotherapies: optimizing outcomes in melanoma. Nat Rev Clin Oncol 2017; 14: 463-482.
[3] Subbiah V, Baik C and Kirkwood JM. Clinical development of BRAF plus MEK inhibitor combinations. Trends Cancer 2020; 6: 797-810.
[4] Eroglu Z and Ribas A. Combination therapy with BRAF and MEK inhibitors for melanoma: latest evidence and place in therapy. Ther Adv Med Oncol 2016; 8: 48-56.
[5] Jenkins RW and Fisher DE. Treatment of advanced melanoma in 2020 and beyond. J Invest Dermatol 2020; 141: 23-31.
[6] Dunker N, Schuster N and Krieglstein K. TGF-beta modulates programmed cell death in the retina of the developing chick embryo. Development 2001; 128: 1933-1942.
[7] Huang SS and Huang JS. TGF-beta control of cell proliferation. J Cell Biochem 2005; 96: 447-462.
[8] Melzer C, von der Ohe J, Hass R and Ungefroren H. TGF-beta-dependent growth arrest and cell migration in benign and malignant breast epithelial cells are antagonistically controlled by Rac1 and Rac1b. Int J Mol Sci 2017; 18: 1574.
[9] Grande JP. Role of transforming growth factor-beta in tissue injury and repair. Proc Soc Exp Biol Med 1997; 214: 27-40.
[10] Travis MA and Sheppard D. TGF-beta activation and function in immunity. Annu Rev Immunol 2014; 32: 51-82.

[11] Syed V. TGF-beta signaling in cancer. J Cell Biochem 2016; 117: 1279-1287.
[12] Schmierer B and Hill CS. TGFbeta-SMAD signal transduction: molecular specificity and functional flexibility. Nat Rev Mol Cell Biol 2007; 8: 970-982.
[13] Hata A and Chen YG. TGF-beta signaling from receptors to smads. Cold Spring Harb Perspect Biol 2016; 8: a022061.
[14] Massague J. TGFbeta signalling in context. Nat Rev Mol Cell Biol 2012; 13: 616-630.
[15] Yan X, Liao H, Cheng M, Shi X, Lin X, Feng XH and Chen YG. Smad7 protein interacts with receptor-regulated smads (R-Smads) to inhibit transforming growth factor-beta (TGF-beta)/smad signaling. J Biol Chem 2016; 291: 382-392.
[16] Wang J, Zhao J, Chu ES, Mok MT, Go MY, Man K, Heuchel R, Lan HY, Chang Z, Sung JJ and Yu J. Inhibitory role of Smad7 in hepatocarcinogenesis in mice and in vitro. J Pathol 2013; 230: 441-452.
[17] Rizzo A, Waldner MJ, Stolfi C, Sarra M, Fina D, Becker C, Neurath MF, Macdonald TT, Pallone F, Monteleone G and Fantini MC. Smad7 expression in T cells prevents colitis-associated cancer. Cancer Res 2011; 71: 7423-7432.
[18] Vignali DA, Collison LW and Workman CJ. How regulatory T cells work. Nat Rev Immunol 2008; 8: 523-532.
[19] Fantini MC, Dominitzki S, Rizzo A, Neurath MF and Becker C. In vitro generation of CD4+ CD25+ regulatory cells from murine naive T cells. Nat Protoc 2007; 2: 1789-1794.
[20] Patterson SJ, Pesenacker AM, Wang AY, Gillies J, Mojibian M, Morishita K, Tan R, Kieffer TJ, Verchere CB, Panagiotopoulos C and Levings MK. T regulatory cell chemokine production mediates pathogenic T cell attraction and suppression. J Clin Invest 2016; 126: 1039-1051.
[21] Ohue Y and Nishikawa H. Regulatory T (Treg) cells in cancer: can treg cells be a new therapeutic target? Cancer Sci 2019; 110: 2080-2089.
[22] French R, Feng Y and Pauklin S. Targeting TGFbeta signalling in cancer: toward context-specific strategies. Trends Cancer 2020; 6: 538-540.
[23] Oh E, Hong J and Yun CO. Regulatory T cells induce metastasis by activating Tgf-beta and enhancing the epithelial-mesenchymal transition. Cells 2019; 8: 1387.
[24] Pang Y, Gara SK, Achyut BR, Li Z, Yan HH, Day CP, Weiss JM, Trinchieri G, Morris JC and Yang L. TGF-beta signaling in myeloid cells is required for tumor metastasis. Cancer Discov 2013; 3: 936-951.
[25] Kudo-Saito C, Shirako H, Takeuchi T and Kawakami Y. Cancer metastasis is accelerated through immunosuppression during Snail-induced EMT of cancer cells. Cancer Cell 2009; 15: 195-206.
[26] Shah AH, Tabayoyong WB, Kundu SD, Kim SJ, Van Parijs L, Liu VC, Kwon E, Greenberg NM and Lee C. Suppression of tumor metastasis by blockade of transforming growth factor beta signaling in bone marrow cells through a retroviral-mediated gene therapy in mice. Cancer Res 2002; 62: 7135-7138.
[27] Zhou C, Li J, Lin L, Shu R, Dong B, Cao D, Li Q and Wang Z. A targeted transforming growth factor-beta (TGF-beta) blocker, TTB, inhibits tumor growth and metastasis. Oncotarget 2018; 9: 23102-23113.
[28] Samanta D and Datta PK. Alterations in the Smad pathway in human cancers. Front Biosci (Landmark Ed) 2012; 17: 1281-1293.
[29] Ullah I, Sun W, Tang L and Feng J. Roles of smads family and alternative splicing variants of smad4 in different cancers. J Cancer 2018; 9: 4018-4028.
[30] Sheen YY, Kim MJ, Park SA, Park SY and Nam JS. Targeting the transforming growth factor-beta signaling in cancer therapy. Biomol Ther (Seoul) 2013; 21: 323-331.
[31] Javelaud D, Mohammad KS, McKenna CR, Fournier P, Luciani F, Niewolna M, Andre J, Delmas V, Larue L, Guise TA and Mauviel A. Stable overexpression of Smad7 in human melanoma cells impairs bone metastasis. Cancer Res 2007; 67: 2317-2324.
[32] Kim S, Han J, Lee SK, Koo M, Cho DH, Bae SY, Choi MY, Kim JS, Kim JH, Choe JH, Yang JH, Nam SJ and Lee JE. Smad7 acts as a negative regulator of the epidermal growth factor (EGF) signaling pathway in breast cancer cells. Cancer Lett 2012; 314: 147-154.
[33] Kobayashi M, Kobayashi H, Pollard RB and Suzuki F. A pathogenic role of Th2 cells and their cytokine products on the pulmonary metastasis of murine B16 melanoma. J Immunol 1998; 160: 5869-5873.
[34] Dobrzanski MJ, Reome JB and Dutton RW. Therapeutic effects of tumor-reactive type 1 and type 2 CD8+ T cell subpopulations in established pulmonary metastases. J Immunol 1999; 162: 6671-6680.
[35] Balkwill FR, Capasso M and Hagemann T. The tumor microenvironment at a glance. J Cell Sci 2012; 125: 5591-5596.
[36] Lindau D, Gielen P, Kroesen M, Wesseling P and Adema GJ. The immunosuppressive tumour network: myeloid-derived suppressor cells, regulatory T cells and natural killer T cells. Immunology 2013; 138: 105-115.
[37] Sarvaria A, Madrigal JA and Saudemont A. B cell regulation in cancer and anti-tumor immunity. Cell Mol Immunol 2017; 14: 662-674.

[38] Cassetta L, Fragkogianni S, Sims AH, Swierczak A, Forrester LM, Zhang H, Soong DYH, Cotechini T, Anur P, Lin EY, Fidanza A, Lopez-Yrigoyen M, Millar MR, Urman A, Ai Z, Spellman PT, Hwang ES, Dixon JM, Wiechmann L, Coussens LM, Smith HO and Pollard JW. Human tumor-associated macrophage and monocyte transcriptional landscapes reveal cancer-specific reprogramming, biomarkers, and therapeutic targets. Cancer Cell 2019; 35: 588-602, e510.

[39] Plitas G and Rudensky AY. Regulatory T cells: differentiation and function. Cancer Immunol Res 2016; 4: 721-725.

[40] Deng G. Tumor-infiltrating regulatory T cells: origins and features. Am J Clin Exp Immunol 2018; 7: 81-87.

[41] Mizukami Y, Kono K, Kawaguchi Y, Akaike H, Kamimura K, Sugai H and Fujii H. CCL17 and CCL22 chemokines within tumor microenvironment are related to accumulation of Foxp3+ regulatory T cells in gastric cancer. Int J Cancer 2008; 122: 2286-2293.

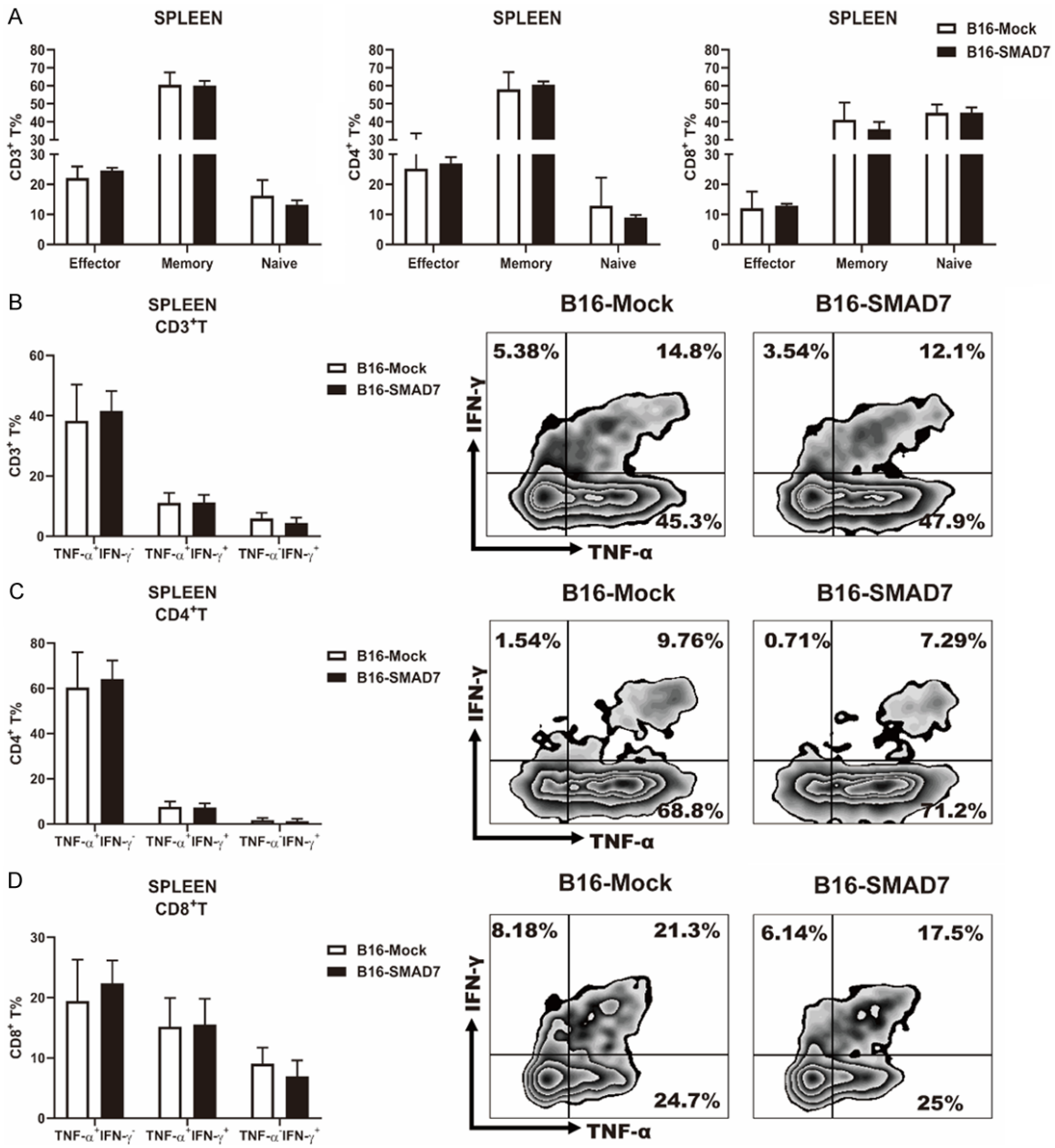

Figure S1. SMAD7 had no influence on T cells distribution and activation in spleen. (A) Splenocytes were isolated from tumor bearing mice 2 weeks after tumor injection. The percentages of $CD44^+CD62L^-$ effector, $CD44^+CD62L^+$ memory and $CD44^-CD62L^+$ naïve T cell subsets were detected by flow cytometry. Representative images of TNF-α^+ IFN-γ^-, TNF-α^+ IFN-γ^+, TNF-α^- IFN-γ^+ (B) $CD3^+$ T cells, (C) $CD4^+$ T cells and (D) $CD8^+$ T cells in the spleen are shown. Data are presented as means ± SD.

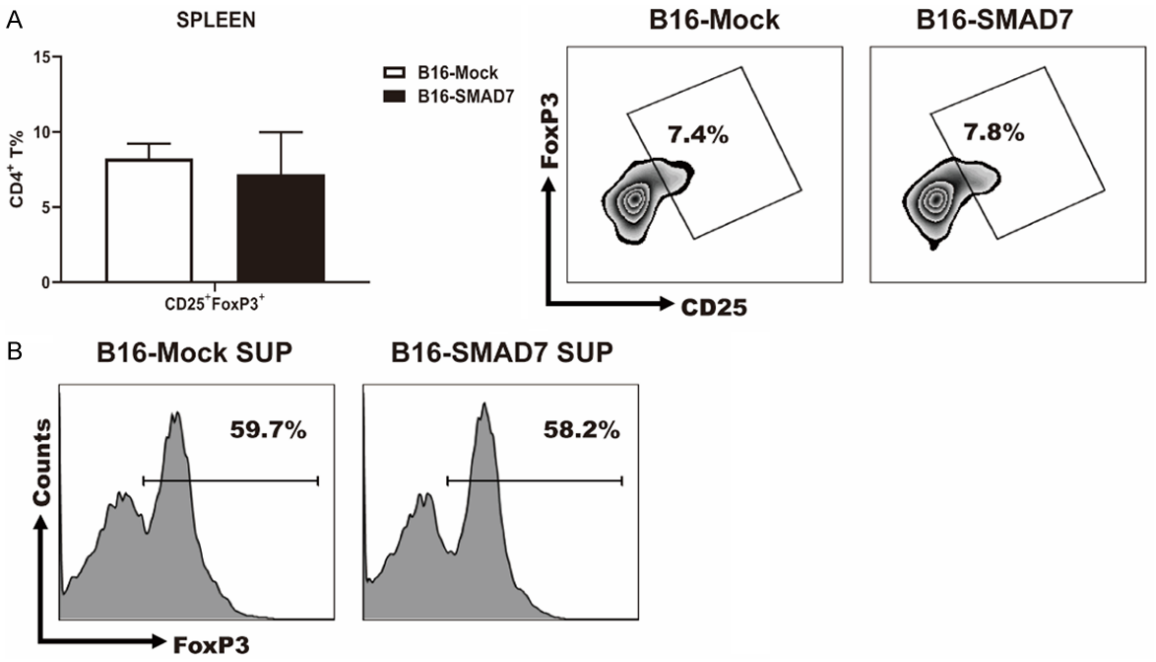

Figure S2. SMAD7 didn't affect Tregs distribution in spleen. A. Representative images of $CD4^+CD25^+FoxP3^+$ Tregs presented in the spleen. B. Representative images of Tregs induced by B16-Mock SUP and B16-SMAD7 SUP. Data are presented as means ± SD.